The American Journal of
PATHOLOGY

ajp.amjpathol.org

GASTROINTESTINAL, HEPATOBILIARY, AND PANCREATIC PATHOLOGY

Hepatic Protein and Phosphoprotein Signatures of Alcohol-Associated Cirrhosis and Hepatitis

Check for updates

Josiah Hardesty,*[†] Le Day,[‡] Jeffrey Warner,*[†] Dennis Warner,* Marina Gritsenko,[‡] Aliya Asghar,[§] Andrew Stolz,[¶] Timothy Morgan,[§] Craig McClain,*[†‖**††] Jon Jacobs,[‡] and Irina Kirpich*[†**††]

From the Division of Gastroenterology, Hepatology, and Nutrition,* Department of Medicine, University of Louisville, Louisville, Kentucky; the Department of Pharmacology and Toxicology,[†] the University of Louisville Alcohol Center,** and the University of Louisville Hepatobiology and Toxicology Center,[††] University of Louisville School of Medicine, Louisville, Kentucky; the Biological Sciences Division and Environmental Molecular Sciences Laboratory,[‡] Pacific Northwest National Laboratory, Richland, Washington; Gastroenterology,[§] VA Long Beach Healthcare, VA Long Beach Healthcare System, Long Beach, California; the Division of Gastrointestinal and Liver Disease,[¶] Department of Medicine, Keck School of Medicine, University of Southern California, Los Angeles, California; and the Robley Rex Veterans Medical Center,[‖] Louisville, Kentucky

Alcohol-associated liver disease is a global health care burden, with alcohol-associated cirrhosis (AC) and alcohol-associated hepatitis (AH) being two clinical manifestations with poor prognosis. The limited efficacy of standard of care for AC and AH highlights a need for therapeutic targets and strategies. The current study aimed to address this need through the identification of hepatic proteome and phosphoproteome signatures of AC and AH. Proteomic and phosphoproteomic analyses were conducted on explant liver tissue (test cohort) and liver biopsies (validation cohort) from patients with AH. Changes in protein expression across AH severity and similarities and differences in AH and AC hepatic proteome were analyzed. Significant alterations in multiple proteins involved in various biological processes were observed in both AC and AH, including elevated expression of transcription factors involved in fibrogenesis (eg, Yes1-associated transcriptional regulator). Another finding was elevated levels of hepatic albumin (ALBU) concomitant with diminished ALBU phosphorylation, which may prevent ALBU release, leading to hypoalbuminemia. Furthermore, altered expression of proteins related to neutrophil function and chemotaxis, including elevated myeloperoxidase, cathelicidin antimicrobial peptide, complement C3, and complement C5 were observed in early AH, which declined at later stages. Finally, a loss in expression of mitochondria proteins, including enzymes responsible for the synthesis of cardiolipin was observed. The current study identified hepatic protein signatures of AC and AH as well as AH severity, which may facilitate the development of therapeutic strategies. (Am J Pathol 2022, 192: 1066−1082; https://doi.org/10.1016/j.ajpath.2022.04.004)

Alcohol-associated liver disease (ALD) is a major health care burden, with alcohol-associated cirrhosis (AC) and alcohol-associated hepatitis (AH) being two major clinical manifestations with frequentl unfavorable outcomes. Globally, liver diseases lead to >2 million deaths per year, with cirrhosis due to excessive alcohol consumption accounting for about one-quarter of them.[1] In 2017, cirrhosis was the 11th leading cause of death in the United States, with 50% of deaths attributed to excessive alcohol use.[2] Binge drinking superimposed on chronic alcohol consumption can cause acute AH in patients with or without preexisting cirrhosis (50% of patients with AH present with cirrhosis[3]). Severe AH is a life-threatening condition, with a 6-month mortality rate reaching 60%,[4] which manifests as jaundice, liver dysfunction, and systemic inflammatory response syndrome.[4,5] The coronavirus disease 2019 (COVID-19) pandemic has further exacerbated this problem, as many states have reported an increase in alcohol sales[6] and alcohol-related hospitalizations,[7] as well as worsened outcomes in COVID-19 patients with alcohol-associated multi-organ pathologies, including ALD.[8] Effective treatment options for severe AH are limited and primarily target the inflammatory response (corticosteroids) or promote liver regeneration and neutrophil production (granulocyte colony-stimulating factor).[9] Clearly, there is an urgent need to develop new treatment strategies to improve long-term survival and quality of life for patients with AC and AH.

Various omic approaches (eg, genomics, transcriptomics, epigenomics, metabolomics/lipidomics, and metagenomics) have been employed to discover novel molecules, pathways, and mechanisms that may facilitate the development of new targeted treatment strategies for ALD. For example, genome-wide association studies found an increased risk of developing AC in patients with the *rs150052* variant of the RNA processing gene *HNRNPUL1*,[10] and an increased risk of both AC and AH in patients with the *rs738409* single-nucleotide polymorphism of the *PNPLA3* gene.[11] Transcriptomic analysis revealed compromised hepatocyte nuclear factor 4α target gene expression, which was associated with hepatocellular failure in AH patients, suggesting that modulation of hepatocyte nuclear factor 4α signaling may improve liver function in AH.[12] Another study using a coupled hepatic transcriptomic and metabolomic analysis revealed an important role of elevated hexokinase domain containing 1 in reprogramming of glucose metabolism in patients with AH and proposed this protein as a potential therapeutic target and biomarker for AH.[13] A lipidomics approach was recently used to discriminate ALD stages based on changes in plasma levels of lipid species (eg, elevated levels of 13-hydroxyoctadecadienoic acid, 9,10-dihydroxyoctadecenoate, and 12,13-dihydroxyoctadecenoate in moderate AH versus heavy drinkers with mild ALD).[14] Because the gut-liver axis plays an important role in ALD, metagenomics has been applied to elucidate microbial/bacterial changes contributing to the disease development/progression (eg, cytolysin-positive *Enterococcus faecalis* was identified as a pathogenic bacterium in clinical AH and successfully targeted in experimental AH[15]). Certainly, omic studies have been invaluable for identifying biomarkers, novel mechanisms, and therapeutic targets for AC and AH. However, to the best of our knowledge, there has been limited characterization of liver proteome signatures for these liver pathologies. Therefore, in the present study, a coupled proteomic and phosphoproteomic analysis was performed to identify alterations in hepatic protein and phosphoprotein levels in patients with AC and AH. Additionally, similarities and differences between these two disease stages were analyzed, and specific proteins, pathways, and mechanisms contributing to the progression of AH severity were identified with the collective goal of identifying novel therapeutic targets to treat these manifestations of ALD.

Materials and Methods

Study Populations and Clinical Characterization

This study analyzed liver samples from two cohorts of patients, which are referred to as the test and validation cohorts (Supplemental Figure S1). The test cohort consisted of de-identified liver samples that were acquired through the University of Louisville and John Hopkins University Clinical Resources Center for Alcoholic Hepatitis Investigations (1R24AA025017-01) and consisted of non-ALD controls ($n = 12$ total, with 7 from University of Louisville and 5 from John Hopkins University) and AH patients ($n = 6$, John Hopkins University) with an average Model for End-Stage Liver Disease (MELD) score of 37.2 ± 1.8. The validation cohort consisted of de-identified liver samples, which were obtained from the Liver Tissue Cell Distribution System at the University of Minnesota (NIH contract HHSN276201200017C; non-ALD controls, $n = 10$; and AC patients, $n = 10$) and the biorepository of the National Institute on Alcohol Abuse and Alcoholism−funded Southern California Alcoholic Hepatitis Consortium (U01AA021884-04; AH patients, $n = 34$). AH patients had an average MELD score of 26 ± 0.8. On the basis of MELD score, AH patients were divided into four groups: AH1 (MELD score, 17 to 20; $n = 4$), AH2 (MELD score, 21 to 25; $n = 14$), AH3 (MELD score, 26 to 29; $n = 11$), and AH4 (MELD score, 30 to 37; $n = 5$). Demographic and clinical characteristics of the study cohorts are provided in Supplemental Tables S1 and S2. All study protocols conformed to the ethical guidelines of the 1975 Declaration of Helsinki, as reflected by the institutional review board approval for the individual studies and acquisition of informed consent from all participating patients. No liver specimens were acquired from executed prisoners or institutionalized persons.

Liver Histology

Formalin-fixed, paraffin-embedded liver samples from AH patients and non-ALD controls were sectioned to a thick-

ness of 5 μm, stained with hematoxylin and eosin, and evaluated by light microscopy at ×200 magnification for gross liver pathology. Liver biopsies were evaluated for AC and AH by expert liver pathologists. Patients were considered to have AH if characteristic features were seen on histology, patients had a history of alcohol abuse, and other liver diseases were excluded. Many patients with AH also had underlying cirrhosis. Patients were diagnosed with AC if they had a history of alcohol abuse that was thought to be the primary cause of their liver disease and no active alcohol-associated steatohepatitis on histology.

Liver Proteome and Phosphoproteome Analysis

Liver proteomic and phosphoproteomic analyses were conducted in the Pacific Northwest National Laboratory using standard protocols and procedures.[16] Test cohort liver sample processing: Approximately 20 to 30 mg of frozen liver tissues were homogenized with a hand-held Tissue-Tearor homogenizer (BioSpec Products, Bartlesville, OK) in 300 μL of lysis buffer (8 mol/L urea, 75 mmol/L NaCl, 50 mmol/L Tris, pH 8.0, and 1 mmol/L EDTA, supplemented with protease and phosphatase inhibitors). Lysates were incubated on ice for 15 minutes and then cleared by centrifugation at $20,000 \times g$ for 10 minutes at 4°C. Protein concentrations were determined by bicinchoninic acid (BCA) assay (Thermo Fisher Scientific, Waltham, MA). Disulfide bonds were reduced with 5 mmol/L dithiothreitol for 1 hour at 37°C and subsequently alkylated with 10 mmol/L iodoacetamide for 45 minutes at 25°C in the dark. Samples were diluted fourfold with 50 mmol/L Tris-HCl, pH 8.0, to obtain a final concentration of 2 mol/L urea before digestion with Lys-C (Wako, Richmond, VA) at a 1:50 enzyme/substrate ratio. After 2 hours of digestion at 25°C, sequencing-grade modified trypsin (Promega, Madison, WI) at 1:50 enzyme/substrate ratio was added to the samples, which were further incubated at 25°C for 14 hours. The reaction was stopped by acidifying the samples with a final concentration of 1% formic acid (Sigma-Aldrich, St. Louis, MO), and samples were centrifuged for 15 minutes at $1500 \times g$. Tryptic peptides were desalted on a C18 SPE cartridge (Waters tC18 SepPak; WAT036820; Milford, MA) and concentrated using a Speed-Vac concentrator. Final peptide concentrations were determined via BCA assay. Peptides (200 μg) were labeled with 10-plex tandem mass tags (TMTs; Thermo Fisher Scientific), according to the manufacturer's recommendations. One of the TMT channels (131) was occupied with a pooled mixture of peptides from all the samples, which serves as a reference to normalize across different sets of samples. Approximately 1.9 mg of 10-plex TMT-labeled sample was separated on a reversed phase Agilent Zorbax 300 Extend-C18 column (250 × 4.6 mm column, containing 3.5-μm particles) using an Agilent 1200 HPLC System (Agilent Technologies, Santa Clara, CA). Solvent A was 4.5 mmol/L ammonium formate, pH 10, and 2% acetonitrile; and solvent B was 4.5 mmol/L ammonium formate, pH 10, and 90% acetonitrile. The flow rate was 1 mL/minute, and the injection volume was 900 μL. TMT-labeled peptides were fractionated into 96 fractions by high-pH reversed-phase chromatography and further concatenated into 24 fractions, as previously described.[17,18] For proteome analysis, 5% of each concatenated fraction was dried down and resuspended in 3% acetonitrile and 0.1% formic acid to a peptide concentration of 0.1 μg/μL for liquid chromatography–tandem mass spectrometry analysis. The rest of the fractions (95%) were further concatenated into 12 fractions, dried down, and subjected to immobilized metal affinity chromatography for phosphopeptide enrichment.

Validation Cohort Liver Sample Processing

Frozen liver biopsies were homogenized for 30 seconds separately in 120 μL of lysis buffer (8 mol/L urea, 75 mmol/L NaCl, 50 mmol/L Tris, pH 8.0, and 1 mmol/L EDTA, supplemented with protease and phosphatase inhibitors) with a Kontes Pellet Pestle Cordless Motor (DWK Life Sciences, Millville, NJ) equipped with a disposable pestle. Lysates were incubated on ice for 15 minutes and were then precleared by centrifugation at $20,000 \times g$ for 10 minutes at 4°C. Protein concentrations were determined by BCA assay (Thermo Fisher Scientific). Protein disulfide bonds were reduced with 5 mmol/L dithiothreitol for 1 hour at 37°C, and then subsequently alkylated with 10 mmol/L iodoacetamide for 45 minutes at 25°C in the dark. Samples were diluted eightfold with 50 mmol/L Tris-HCl, pH 8, and sequencing-grade modified trypsin (Promega) at a 1:50 enzyme/substrate ratio was added to the samples and digested at 37°C for 4 hours.

Phosphopeptide Enrichment

Fe^{3+}-NTA-agarose beads were freshly prepared using the Ni-NTA Superflow agarose beads (Qiagen, Hilden, Germany) for phosphopeptide enrichment. For each of the 12 fractions, peptides were reconstituted to 0.5 μg/μL in immobilized metal affinity chromatography binding/wash buffer (80% acetonitrile and 0.1% trifluoroacetic acid) and incubated with 10 μL of the Fe^{3+}-NTA-agarose beads for 30 minutes at room temperature. After incubation, the beads were washed two times each with 50 μL of wash buffer and once with 50 μL of 1% formic acid on the stage tip packed with 2 discs of Empore C18 material (Empore Octadecyl C18, 47 mm; 98-0604-0217-3; CDS Analytical, Northlake, IL). Phosphopeptides were eluted with 70 μL Elution Buffer (500 mmol/L potassium phosphate buffer). Phosphopeptides were then eluted from the C18 stage tips with 50% acetonitrile and 0.1% formic acid. Samples were dried using a Speed-Vac concentrator (Thermo Fisher Scientific), and then reconstituted with 12 μL of 3% acetonitrile and 0.1% formic acid for liquid chromatography–tandem mass spectrometry analysis. The samples were acidified in 1% formic acid (Sigma-Aldrich) and centrifuged for 15 minutes at $1500 \times g$ to clear the digest of precipitated material. Tryptic peptides were desalted on a C18 SPE (Waters tC18

SepPak; WAT036820) and concentrated using a Speed-Vac concentrator. The final peptide concentration was determined via BCA assay.

Liquid Chromatography—Tandem Mass Spectrometry

Global- and phosphopeptide-enriched samples were subjected to a custom high mass accuracy liquid chromatography—tandem mass spectrometry system, as previously described,[19] where the liquid chromatography component consisted of automated reversed-phase columns prepared in-house by slurry packing 3 μm Jupiter C18 (Phenomenex) into 35 cm × 360 μm o.d. × 75 μm i.d. fused silica (Polymicro Technologies Inc., Phoenix, AZ). The mass spectrometry component consisted of a Q Exactive HF Hybrid Quadrupole-Orbitrap mass spectrometer (Thermo Fisher Scientific) outfitted with a custom electrospray ionization interface. Electrospray emitters were custom made using 360 μm o.d. × 20 μm i.d. chemically etched fused silica capillary tubes. Analysis of the phosphoproteome samples applied similar conditions as used in the global proteome sample analysis. All other instrument conditions were set as previously described.[19]

Mass Spectrometry

The key search parameters used were 20 parts per million tolerance for precursor ion masses, 2.5 and −1.5 Da window on fragment ion mass tolerances, no limit on missed cleavages, partial tryptic search, no exclusion of contaminants, dynamic oxidation of methionine (15.9949 Da), static iodoacetamide alkylation on cysteine (57.0215 Da), and static TMT modification of lysine and N-termini (144.1021 Da). The decoy database searching method[20,21] was used to control the false discovery rate at the unique peptide level to <0.01% and subsequent protein level to <0.1%.[22] Quantification was based on initially summing to the protein level the sample-specific peptide reporter ion intensities captured for each channel across all 12 analytical fractions. Final data for statistical analysis were the ratio of each protein summed value with the pooled reference control within each TMT10 experiment to adjust for experiment-specific variability. All proteomic and phosphoproteomic data sets are deposited in the MassIVE repository (accession number MSV000089168; *https://massive.ucsd.edu/ProteoSAFe/static/massive.jsp*, last accessed March 31, 2022).

Cytoscape Protein Clustering, GO, and STEM

Hepatic proteins that were significantly differentially expressed between controls and AH in the test cohort ($P < 0.05$) were analyzed in Cytoscape via Gene Ontology (GO) analysis to identify specific biological processes associated with those proteins.[23] GO processes that met the false discovery rate of 0.05 were used for further analysis. Similarly, proteins that met the previous criteria were analyzed by MCL Cluster Analysis in

Cytoscape. Protein String figures of processes were generated in Cytoscape.[23] Short time-series expression miner (STEM) analysis[24] was conducted on the average protein expression for AH1 to AH4 patient groups to identify protein expression patterns that changed with AH severity. Significant STEM protein clusters were used to identify GO Processes associated with proteins within that cluster.

Western Blot

Liver tissue samples from non-ALD control ($n = 5$) and AH patients ($n = 6$; test cohort) were homogenized in radio-immunoprecipitation assay buffer (10 mmol/L Tris-HCl, pH 8.0, 1 mmol/L EDTA, 0.5 mmol/L EGTA, 1% Triton X-100, 0.1% sodium deoxycholate, 0.1% SDS, and 140 mmol/L NaCl) supplemented with HALT protease and phosphatase inhibitors (Thermo Fisher Scientific), followed by centrifugation for 10 minutes at $16,000 \times g$. Protein concentrations were determined by the BCA (Pierce BCA protein assay kit; Thermo Fisher Scientific). A total of 30 μg of protein was separated on Criterion TGX Any kDa gels (BioRad, Hercules, CA) and then transferred to polyvinylidene difluoride membranes and blocked in 5% milk Tris-buffered saline + 0.1% Tween-20. Membranes were incubated overnight at 4°C with primary antibodies (1:1000 dilution in 5% bovine serum albumin Tris-buffered saline + 0.1% Tween-20), thoroughly washed, and then incubated with secondary antibodies at 1:2000 dilution in 5% milk Tris-buffered saline + 0.1% Tween-20 at room temperature for 1 hour and washed; and signals were developed with enhanced chemiluminescence substrate (Clarity Max; BioRad) and imaged via the ChemiDoc instrument (BioRad). Band densitometry analysis was conducted with ImageLab software version 6.0.1 (BioRad). The primary antibodies used included S61—Yes1-associated transcriptional regulator (YAP1), YAP1, ALBU, and β-actin (Cell Signaling Technology, Danvers, MA), and the secondary antibody used was a horseradish peroxidase—conjugated goat anti-rabbit IgG antibody (Thermo Fisher Scientific).

Liver Cardiolipin Assay

A total of 10 μg of liver protein extract was used from non-ALD control liver ($n = 15$), AC ($n = 7$), and AH ($n = 6$). Liver cardiolipin levels were measured using a fluorometric assay kit (Abcam, Cambridge, MA).

Statistical Analysis

All continuous variables are presented as means ± SEM. Data between two groups were compared by unpaired *t*-test, and data between multiple groups were compared by one-way analysis of variance using InfernoRDN software v1.1.7995 (*https://www.pnnl.gov/integrative-omics*, last accessed May 14, 2021). Linear correlation analysis was conducted between individual proteins and clinical parameters in R
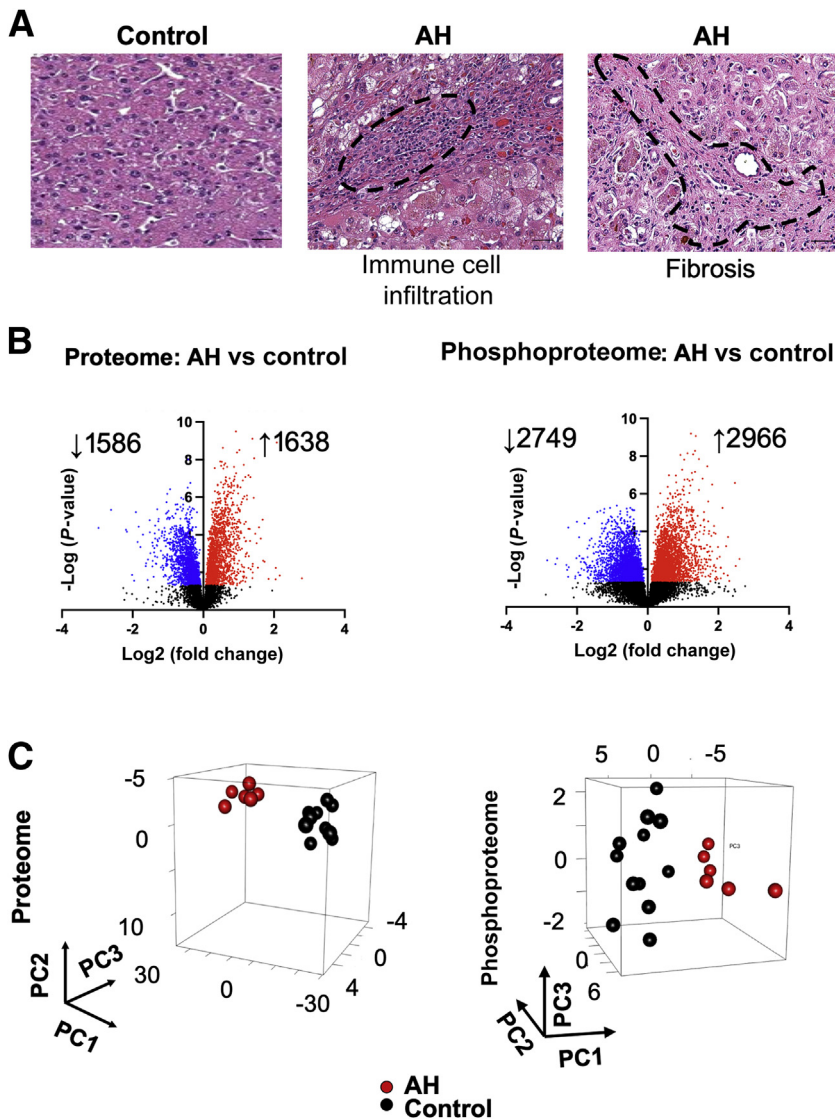
Figure 1 Alterations of hepatic proteins in the alcohol-associated hepatitis (AH) test cohort identified by proteomic analysis. **A:** Representative hematoxylin and eosin—stained liver sections. Immune cell infiltrate and fibrotic areas are outlined (**dashed black lines**) in the representative histologic images. **B:** Volcano plot analysis of the hepatic proteome and phosphoproteome (blue and red colors denote significantly decreased or increased proteins, respectively; $P < 0.05$). **C:** Principal component (PC) analysis of proteome and phosphoproteome. Scale bar = 50 μm (**A**). Original magnification, ×200 (**A**).

version 4.0.3. (*https://www.r-project.org*, last accessed March 3, 2021). $P < 0.05$ was considered significant for all statistical tests. Receiver operating characteristic analysis and principal component analysis were conducted in GraphPad Prism version 9.1.0 (GraphPad Software, San Diego, CA). Principal component scores were then visualized via RStudio Software version 1.3.1093 (RStudio, Boston, MA) using the plot3D function of the rgl package.

Results

Alterations of Hepatic Proteins and Biological Processes in AH Test Cohort Identified by Proteomic Analysis

Initially, explant liver tissue samples from the AH test cohort (characterized by typical histopathologic features of AH) (Figure 1A) were used to identify changes in protein expression, which were investigated further in an independent AH validation cohort. Hepatic proteomic analysis revealed significant differences in numerous proteins (1586 decreased and 1638 increased) and phosphoproteome (2749 decreased phosphopeptides and 2966 increased phopshopeptides) between AH and controls (Figure 1, B and C). The top proteins decreased in AH included the following metabolic enzymes: glutathione S-transferase alpha 1 (GSTA1; −7.8-fold), alcohol dehydrogenase 4 (ADH4; −6.1-fold), alcohol dehydrogenase 1A (ADH1A; −4.6-fold), glutathione S-transferase alpha 2 (GSTA2; −3.9-fold), and alcohol dehydrogenase 6 (ADH6; −3.8-fold); the top proteins increased were: A-kinase anchoring protein 17A (AK17A; 6.9-fold), heat shock 70 KDa protein 1L (HS71L; 4.2-fold), calpain 6 (CAN6; 3.6-fold), keratin 19 (K1C19; 3.3-fold), and zinc finger protein 512 (ZN512; 3.2-fold) (Supplemental Table S3). The changes in the phosphoproteome levels are presented in Supplemental Table S4. GO processes that were significantly increased in AH included mRNA processing, transcription, fibrosis, neutrophils, and extracellular matrix,

Table 1 AH Validation Cohort Demographic Information

AH group	Sex	Age, years	Survival 24 weeks	MDF score	MELD score
AH1 (n = 4)	M	45	Y	27	17
	M	50	Y	20	18
	F	24	Y	41	18
	M	32	?	35	20
AH2 (n = 14)	M	32	Y	35	21
	F	43	?	43	21
	M	31	Y	38	22
	M	65	Y	34	23
	M	57	Y	34	23
	M	27	Y	33	23
	M	38	N	48	24
	M	58	Y	41	24
	M	59	Y	43	24
	M	51	Y	37	24
	M	54	N	31	25
	M	65	Y	48	25
	M	57	Y	47	25
	M	45	Y	59	25
AH3 (n = 11)	F	34	Y	66	26
	M	48	Y	60	26
	M	28	?	72	26
	M	39	?	72	27
	M	39	N	75	28
	M	26	N	99	28
	M	44	Y	58	28
	M	39	Y	65	29
	M	43	Y	90	29
	M	38	?	67	29
	M	43	N	57	29
AH4 (n = 5)	M	26	Y	101	30
	M	30	?	61	32
	M	50	N	33	32
	M	41	?	64	35
	M	36	?	87	37

F, female; M, male; AH, alcohol-associated hepatitis; MDF, Maddrey discriminant function; MELD, Model for End-Stage Liver Disease; N, no; Y, yes.

among others (Supplemental Figure S2A). Clusters of proteins diminished in AH included proteostasis, tRNA, translation, mitochondrial translation, and metabolism (Supplemental Figure S2B).

Hepatic Proteomic Changes in AH Validation Cohort and AC Patients

To confirm findings in the test cohort, the study analyzed liver biopsy samples from a validation cohort consisting of AH patients stratified into four severity groups by MELD score (Table 1). In addition, liver biopsy samples from patients with AC were analyzed to identify proteomic similarities and differences between patients with AH and AC. Principal component analysis plots demonstrated a clear differentiation between patients with AC and AH based on their respective hepatic proteome and phosphoproteome (Figure 2A). Proteomic analysis revealed that the expression of 4738 proteins (2250 decreased and 2488 increased) and 4542 phosphopeptides (2147 decreased and 2395 increased) was significantly different between AH validation cohort and controls (Figure 2B). The proteins with the greatest decrease in expression in this cohort that were also reduced in the test cohort were GSTA1, ADH4, ADH1A, GSTA2, and ADH6, whereas the proteins most elevated in both cohorts included AK17A, HS71L, CAN6, K1C19, and ZN512 (Supplemental Table S5). The changes in the phosphopeptide levels are presented in Supplemental Table S6. The proteome and phosphoproteome changes in AC versus control are listed in Supplemental Tables S5 and S6, respectively. When comparing AH with AC, 3006 proteins (1763 decreased and 1243 increased) and 4451 phosphopeptides (2213 decreased and 2238 increased) were significantly different (Figure 2C). The top proteins that decreased in AH versus AC included trypsin-1 (TRY1; −5.0-fold), keratin 80 (K2C80; −3.3-fold), dehydrogenase/reductase 4 like 2 (DR4L2; −3.1-fold), serpin family B member 7 (SPB7; −2.7-fold), and nerve growth factor (NGF; −2.6-fold); the top increased were H2B clustered histone 11 (H2B1J; 9.8-fold), poly (A) binding protein cytoplasmic 4 like (PAB4L; 3.6-fold), H2B clustered histone 4 (H2B1C; 3.2-fold), ATP synthase F1 subunit epsilon (ATP5E; 3.1-fold), and histocompatibility antigen, B-73 (1B73; 3-fold) (Supplemental Table S5). The changes in the phosphopeptide levels are presented in Supplemental Table S6. GO Process analysis revealed the top decreased processes in AH relative to AC, which included cell matrix adhesion, oxidative phosphorylation, and proteasomal degradation. The most up-regulated processes in AH versus AC were related to transcription, acute-phase proteins (APPs), and neutrophil function (Supplemental Table S7). Finally, to identify patterns in protein expression, STEM analysis was conducted, followed by GO Process analysis, resulting in the separation of STEM profiles into two groups (reduced and increased in AH1 to AH4 versus controls) (Figure 2D). The expression of proteins involved in amino acid metabolism declined with AH severity. In contrast, the expression of mRNA processing proteins increased with AH severity.

Up-Regulated Hepatic YAP1 Expression Is Associated with Compromised YAP1 Phosphoregulation in AC and AH

Because processes related to transcription were affected in both AH cohorts (Supplemental Figure S2), the study aimed to identify alterations in the expression of transcription factors (TFs), as these proteins are significant regulators of transcription. Among the 40 total TFs analyzed, 26 were similarly changed in both AH cohorts versus controls (9 decreased and 17 increased) (Table 2 and Figure 3A). When comparing AH and AC versus controls, 19 similarly changed TFs were observed (7 decreased and 12 increased), and there were 16 differentially expressed TFs between the
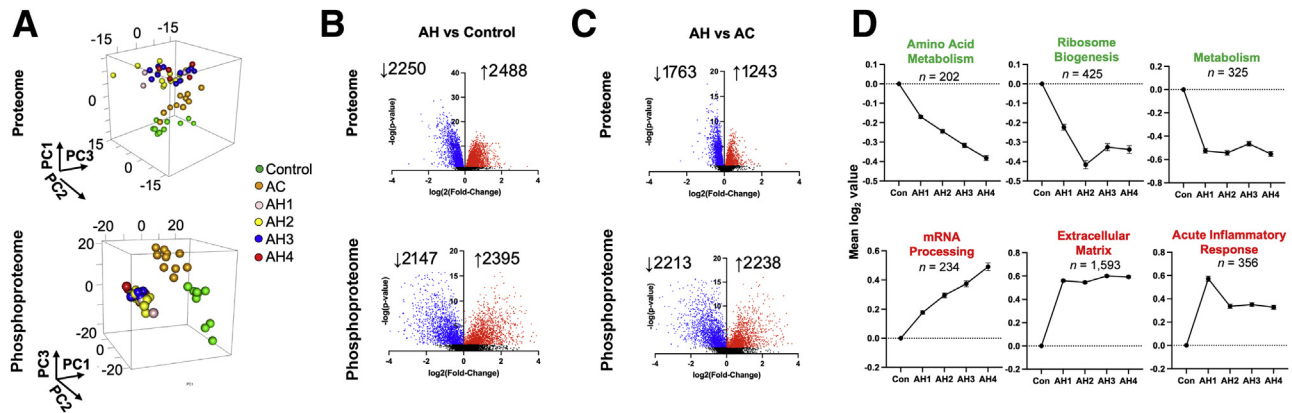
Figure 2 Hepatic proteomic changes in alcohol-associated hepatitis (AH) validation cohort and patients with alcohol-associated cirrhosis (AC). **A:** Principal component (PC) analysis of proteome and phosphoproteome in patients with AH and AC. **B** and **C:** Volcano plot analysis of the proteome and phosphoproteome for patients with AH versus controls and for patients with AH versus AC, respectively (blue and red colors denote significantly decreased or increased proteins, respectively; $P < 0.05$). **D:** Short time-series expression miner (STEM) cluster analysis demonstrating patterns of protein expression for the identified Gene Ontology (GO) processes across AH severity. n, number of proteins within each GO process.

two groups. Of note, four TFs that were significantly increased in both AH cohorts also had significant positive associations with MELD score [AE binding protein 1 (AEBP1), Pearson $r = 0.5043$, $P = 0.002$] or Maddrey discriminant function score [YAP1, $r = 0.3774$, $P = 0.03$; AEBP1, $r = 0.7374$, $P = 6.5 \times 10^{-7}$; methyl CpG binding protein 2 (MECP2), $r = 0.4146$, $P = 0.02$; and nuclear receptor subfamily 2 group F member 2 (NR2F2), $r = 0.4606$, $P = 0.006$] (Supplemental Table S8). Furthermore, receiver operating characteristic curve analysis determined that the expression of a set of TFs could differentiate AH severity groups, with the distinction between AH2 and AH3 being the most significant (Figure 3B). This differentiation between AH2 and AH3 is noteworthy because patients in the AH3 severity group (MELD score, 26 to 29) have a predicted 3-month mortality rate of 47% to 58%, compared with 28% to 43% for AH2 (MELD score, 21 to 25).[25] In addition, nuclear receptor subfamily 2 group F member 1 (NR2F1) expression was significantly higher in AH nonsurvivors versus survivors (Supplemental Table S9). Of interest, elevated YAP1 has been previously implicated in AH pathogenesis,[26] but the mechanisms governing its aberrant activity have not been determined. Herein, YAP1 phosphorylation was examined as a potential mechanism of its regulation. Findings from both AH cohorts demonstrated decreased pS61-YAP1, a phosphorylation mark that represses YAP1 activity,[27] and elevated pS105-YAP1, a phosphorylation mark whose function is yet to be determined (Figure 3C and Supplemental Tables S10 and S11). Western blot analysis confirmed these results in liver tissue samples from the AH test cohort (Supplemental Figure S3, A and B). As in patients with AH, pS61-YAP1 was also reduced in patients with AC. In addition, pS382-YAP1 was decreased, and pS127-YAP1, a marker of YAP1 degradation,[27] was elevated in only AH validation cohort versus controls. When comparing AH with AC, levels of pS382-

YAP1 were lower, whereas pS105-YAP1 and pS127-YAP1 were higher, in AH versus AC (Figure 3C). To further evaluate YAP1 transcriptional activity, expression levels of the YAP1 co-activator WW domain containing transcription regulator (TAZ), as well as YAP target genes were examined. The expression of TAZ was unchanged, whereas the expression of YAP1 target genes laminin subunit beta 2 (LAMB2), Notch receptor 2 (NOTC2), and insulin-like growth factor binding protein 3 (IBP3) was increased relative to controls in the AH validation cohort (Figure 3D) and test cohort (Supplemental Figure S3C), with the exception of IBP3. YAP1 target genes were also elevated in AC versus controls; however, only IBP3 and LAMB2 were higher in AC versus AH. Across AH severity, expression of YAP1/TAZ target genes generally mirrored YAP1 expression (Figure 3E). Several YAP1 phosphorylation sites were positively (pS61, pS109, pS127, pS163, pS164, and pS382) or negatively (pS105, pT63, and pT110) associated with MELD score (Figure 3F). Overall, these data demonstrated that YAP1 expression and activity were elevated in AC and AH, possibly due to disruption of phosphoregulation.

Elevated Liver MECP2 Protein Levels Are Associated with Reduced Phosphorylation in AH

The TFs mentioned above (AEBP1, MECP2, NR2F1, and NR2F2) were investigated further along with their target genes and regulation. Target genes of AEBP1 [fibulin-3 (FBLN3) and asporin (ASPN)], MECP2 [TRIO and F-actin binding protein (TARA) and desmin (DESM)], NR2F1 [fatty acid binding protein 5 (FABP5)], and NR2F2 [laminin subunit beta 1 (LAMB1)] were elevated in both AH cohorts and AC relative to controls (Table 2). Target genes of AEBP1 and NR2F2, but not NR2F1 or MECP2, were positively associated with MELD score (FBLN3, Pearson

Table 2   Specific Hepatic Proteome Changes in AH and AC

Variable	Protein	Test cohort					Validation cohort								
		Con		AH		Con vs AH	Con		AC		AH		Con vs AC	Con vs AH	AC vs AH
		Mean	SD	Mean	SD	P value	Mean	SD	Mean	SD	Mean	SD	P value		
Transcription factors	HMGA1	1.00	0.18	1.66	0.31	<0.0001	0.86	0.16	1.29	0.22	1.64	0.35	0.0001	<0.0001	0.004585
	NR2F2	1.00	0.15	1.51	0.27	<0.0001	0.86	0.29	1.91	0.44	1.40	0.27	<0.0001	<0.0001	<0.0001
	AEBP1	1.05	0.17	1.55	0.17	<0.0001	0.92	0.08	1.28	0.16	1.63	0.28	<0.0001	<0.0001	0.0006
	NC2B	1.05	0.23	1.49	0.27	0.0024	1.15	0.31	1.43	0.32	1.46	0.29	0.0609	0.0041	0.7199
	ZNF24	1.13	0.10	1.57	0.17	0.0014	1.38	0.60	1.28	0.16	1.48	0.24	0.6835	0.4772	0.0374
	GLMP	1.00	0.19	1.38	0.18	0.0009	0.89	0.27	1.07	0.10	1.64	0.74	0.0997	0.0054	0.0357
	HNF1B	1.07	0.18	1.44	0.50	0.0290	1.67	0.45	1.62	0.24	1.53	0.38	0.7994	0.3951	0.5328
	NFKB2	1.09	0.14	1.46	0.06	<0.0001	1.42	0.26	1.45	0.12	1.40	0.12	0.7270	0.7094	0.2180
	NR2F1	1.05	0.10	1.39	0.29	0.0016	1.03	0.17	1.59	0.20	1.47	0.24	<0.0001	<0.0001	0.1679
	NC2A	1.12	0.07	1.46	0.21	<0.0001	1.02	0.23	1.30	0.18	1.61	0.36	0.0082	<0.0001	0.0137
	ATF7	1.06	0.14	1.38	0.13	<0.0001	1.13	0.26	1.36	0.25	1.39	0.19	0.0829	0.0041	0.7704
	MECP2	1.10	0.09	1.43	0.16	<0.0001	1.07	0.12	1.71	0.32	1.53	0.44	<0.0001	0.0023	0.2508
	T22D1	1.16	0.17	1.50	0.18	0.0014	1.15	0.20	1.56	0.21	1.42	0.24	0.0003	0.0021	0.0991
	RARA	1.09	0.12	1.39	0.19	0.0008	1.21	0.18	1.40	0.22	1.57	0.19	0.0762	<0.0001	0.0284
	PURB	1.12	0.16	1.38	0.15	0.0041	1.21	0.07	1.41	0.15	1.51	0.17	0.0013	<0.0001	0.0988
	BPTF	1.20	0.17	1.45	0.08	0.0474	1.08	0.07	1.51	0.49	1.35	0.22	0.0821	0.0140	0.2841
	NFKB1	1.13	0.07	1.35	0.08	<0.0001	1.30	0.10	1.50	0.09	1.47	0.15	0.0002	0.0013	0.6308
	YAP1	1.12	0.11	1.33	0.12	0.0026	1.26	0.16	1.61	0.32	1.48	0.21	0.0059	0.0043	0.1319
	SP3	1.15	0.14	1.31	0.10	0.0302	1.11	0.17	1.61	0.12	1.69	0.39	0.0004	0.0027	0.6823
	TF65	1.16	0.10	1.28	0.12	0.0365	1.49	0.25	1.63	0.19	1.40	0.13	0.1899	0.1347	<0.0001
	STAT6	1.17	0.06	1.27	0.08	0.0062	1.30	0.09	1.60	0.11	1.46	0.10	<0.0001	<0.0001	0.0004
	NFAC2	1.13	0.26	1.15	0.08	0.8858	1.08	0.28	1.25	0.16	1.47	0.28	0.2038	0.0062	0.0627
	CEBPB	1.22	0.12	1.12	0.11	0.1281	1.23	0.28	1.28	0.16	1.63	0.25	0.6778	0.0023	0.0011
	NR1H4	1.17	0.16	1.06	0.12	0.1930	1.15	0.23	1.22	0.17	1.40	0.18	0.5857	0.0184	0.0384
	SMAD4	1.24	0.12	1.09	0.10	0.0227	1.47	0.22	1.39	0.23	1.57	0.29	0.4553	0.2965	0.0749
	NFIC	1.23	0.12	1.05	0.15	0.0139	1.45	0.13	1.72	0.20	1.33	0.09	0.0019	0.0014	<0.0001
	PREB	1.26	0.16	1.07	0.10	0.0204	1.31	0.07	1.26	0.10	1.57	0.19	0.2513	0.0001	<0.0001
	NKRF	1.17	0.07	0.99	0.15	0.0384	1.98	0.64	1.88	0.70	2.04	1.41	0.7855	0.9255	0.7636
	STAT3	1.29	0.16	1.08	0.13	0.0146	1.92	0.27	1.50	0.14	1.29	0.08	0.0003	<0.0001	<0.0001
	FOXA3	1.09	0.35	0.91	0.24	0.4561	1.40	0.13	1.61	0.11	1.41	0.48	0.0657	0.9634	0.4348
	NR1I2	1.14	0.15	0.92	0.08	0.0538	1.82	0.25	1.35	0.35	1.32	0.18	0.1285	0.0013	0.8624
	HNF4a	1.26	0.07	1.02	0.07	<0.0001	1.30	0.30	1.41	0.16	1.47	0.35	0.3064	0.1736	0.6256
	PROX1	1.32	0.17	1.06	0.05	0.0021	1.69	0.16	1.42	0.13	1.43	0.13	0.0006	<0.0001	0.8404
	ZBT20	1.34	0.18	1.01	0.23	0.0034	1.51	0.27	1.43	0.14	1.40	0.19	0.4708	0.1529	0.5817
	ZN787	1.38	0.13	1.04	0.03	0.0026	0.98	0.30	1.22	0.21	1.33	0.16	0.0648	<0.0001	0.0606
	ANDR	1.32	0.37	0.95	0.39	0.0693	2.65	0.59	1.55	0.22	1.22	0.21	0.0096	<0.0001	0.0137
	RXRA	1.33	0.22	0.91	0.05	0.0003	1.83	0.59	1.33	0.13	1.32	0.23	0.0164	0.0002	0.9970
	HNF1A	1.29	0.25	0.86	0.13	0.0014	1.87	0.32	1.37	0.17	1.32	0.29	0.0003	<0.0001	0.6290
	MLXPL	1.56	0.26	0.98	0.24	0.0003	2.48	0.63	1.26	0.20	1.14	0.22	0.0033	<0.0001	0.2940
	MLX	1.51	0.37	0.77	0.13	0.0003	2.19	0.54	1.53	0.20	1.25	0.14	0.0020	<0.0001	<0.0001
AEBP1	ASPN	0.97	0.26	1.74	0.63	0.0019	0.78	0.16	1.75	0.77	1.42	0.35	0.0010	<0.0001	0.0590
	FBLN3	0.87	0.24	1.86	0.32	0.0000	0.90	0.22	2.01	0.45	1.45	0.23	<0.0001	<0.0001	<0.0001
MECP2	DESM	0.98	0.73	1.69	0.36	0.0421	0.76	0.15	1.36	0.24	1.61	1.01	<0.0001	0.0115	0.4371
	TARA	1.13	0.10	1.30	0.13	0.0060	1.10	0.11	1.41	0.13	1.60	0.17	<0.0001	<0.0001	0.0014
NR2F1	FABP5	0.95	0.20	1.95	0.45	<0.0001	1.06	0.10	1.49	0.27	1.55	0.28	<0.0001	<0.0001	0.5221
	ZBT16	1.19	0.29	0.88	0.13	0.0235	1.84	0.57	1.40	0.18	1.43	0.34	0.1812	0.0570	0.8387
NR2F2	ANGL4	1.25	0.21	1.28	0.16	0.8031	1.23	0.07	1.64	0.35	1.38	0.19	0.0044	0.0362	0.0064
	LAMB1	0.91	0.20	1.76	0.32	<0.0001	0.94	0.10	1.45	0.20	1.60	0.27	<0.0001	<0.0001	0.1003

(table continues)

Table 2 (*continued*)

Variable	Protein	Test cohort Con Mean	SD	AH Mean	SD	Con vs AH P value	Validation cohort Con Mean	SD	AC Mean	SD	AH Mean	SD	Con vs AC P value	Con vs AH	AC vs AH
Protein synthesis process	SYIC	1.24	0.12	1.11	0.07	0.0386	1.60	0.11	1.46	0.07	1.39	0.10	0.0045	<0.0001	0.0365
	SYVC	1.21	0.08	1.24	0.11	0.4575	1.44	0.10	1.49	0.15	1.43	0.09	0.4960	0.6452	0.1481
	SYEP	1.23	0.10	1.15	0.10	0.1203	1.50	0.12	1.49	0.08	1.44	0.07	0.6883	0.0479	0.0999
	SYMC	1.24	0.11	1.17	0.11	0.2132	1.51	0.15	1.40	0.09	1.43	0.08	0.0643	0.0372	0.3224
	SYSC	1.26	0.10	1.03	0.13	0.0005	1.89	0.19	1.60	0.11	1.33	0.09	0.0006	<0.0001	<0.0001
	SYRC	1.27	0.09	1.11	0.10	0.0035	1.63	0.15	1.57	0.12	1.37	0.11	0.2963	<0.0001	<0.0001
	MCA3	1.21	0.13	1.21	0.11	0.9552	1.39	0.13	1.47	0.11	1.57	0.32	0.1693	0.0934	0.3403
	GARS	1.23	0.16	1.12	0.13	0.1809	1.56	0.24	1.41	0.11	1.41	0.15	0.0795	0.0179	0.9800
	AIMP2	1.31	0.16	1.08	0.13	0.0088	1.49	0.20	1.61	0.22	1.42	0.09	0.2536	0.0972	0.0003
	SYNC	1.20	0.14	1.21	0.07	0.9471	1.14	0.15	1.33	0.16	1.58	0.19	0.0133	<0.0001	0.0006
	SYFB	1.20	0.15	1.12	0.10	0.2557	1.48	0.16	1.55	0.10	1.36	0.10	0.2684	0.0052	<0.0001
	SYQ	1.26	0.11	1.10	0.05	0.0049	1.54	0.11	1.52	0.11	1.39	0.09	0.7354	0.0001	0.0006
	SYTC	1.24	0.08	1.10	0.08	0.0049	1.72	0.19	1.63	0.29	1.32	0.09	0.4208	<0.0001	<0.0001
	SYAC	1.25	0.10	1.11	0.05	0.0033	1.78	0.24	1.55	0.12	1.38	0.12	0.0146	<0.0001	0.0003
	AIMP1	1.23	0.08	1.20	0.09	0.4648	1.40	0.14	1.53	0.15	1.48	0.15	0.0582	0.1282	0.3718
	MK14	1.15	0.07	1.28	0.10	0.0064	1.48	0.10	1.59	0.15	1.45	0.17	0.0891	0.6357	0.0356
	MP2K3	1.23	0.13	1.18	0.05	0.3568	1.46	0.15	1.53	0.07	1.38	0.14	0.2366	0.1438	0.0037
	M3K5	ND	ND	ND	ND	ND	1.59	0.17	1.63	0.27	1.22	0.12	0.7915	<0.0001	<0.0001
	MKNK1	ND	ND	ND	ND	ND	0.90	0.39	0.92	0.37	1.68	0.96	0.9264	0.0165	0.0185
	BRAF	1.27	0.07	1.27	0.10	0.9794	1.67	0.15	1.56	0.16	1.36	0.16	0.1407	<0.0001	0.0016
	MP2K1	1.15	0.12	1.08	0.09	0.2599	1.71	0.23	1.51	0.20	1.39	0.21	0.0561	0.0002	0.1136
	MK01	1.19	0.08	1.31	0.11	0.0210	1.22	0.14	1.49	0.22	1.56	0.25	0.0053	0.0002	0.4132
	KS6A1	1.17	0.07	1.33	0.05	<0.0001	1.32	0.14	1.46	0.12	1.44	0.13	0.0268	0.0127	0.6914
	IF4G1	1.32	0.19	1.03	0.04	0.0020	1.80	0.16	1.46	0.19	1.34	0.08	0.0005	<0.0001	0.0084
	IF4A1	1.24	0.20	1.20	0.18	0.6808	1.81	0.23	1.47	0.16	1.39	0.12	0.0012	<0.0001	0.1184
	IF4A2	1.20	0.13	1.12	0.15	0.2823	1.69	0.17	1.34	0.09	1.45	0.11	<0.0001	<0.0001	0.0074
	EF2	1.30	0.29	1.11	0.12	0.1292	1.94	0.26	1.48	0.11	1.34	0.07	<0.0001	<0.0001	<0.0001
	EF2K	1.08	0.23	1.08	0.25	0.9529	1.19	0.31	1.30	0.20	1.51	0.26	0.4586	0.0111	0.0819
	RS6	1.25	0.34	1.12	0.20	0.3835	1.37	0.15	1.37	0.11	1.54	0.17	0.9131	0.0047	0.0047
	IF4B	1.30	0.12	1.10	0.06	0.0018	1.49	0.23	1.50	0.18	1.51	0.19	0.9669	0.8187	0.8205
	SYIM	1.27	0.12	1.09	0.09	0.0055	1.72	0.13	1.47	0.10	1.38	0.14	0.0001	<0.0001	0.0721
	SYEM	1.27	0.16	1.05	0.09	0.0062	1.57	0.18	1.33	0.16	1.45	0.20	0.0044	0.0968	0.0841
	SYRM	1.29	0.17	1.17	0.24	0.2312	1.68	0.24	1.44	0.23	1.30	0.14	0.0393	<0.0001	0.0215
	SYNM	1.33	0.12	1.00	0.13	<0.0001	1.63	0.26	1.40	0.23	1.35	0.20	0.0556	0.0007	0.4706
	SYVM	1.15	0.24	1.00	0.17	0.1865	1.64	0.18	1.35	0.13	1.41	0.17	0.0005	0.0006	0.2643
	SYPM	1.23	0.15	1.11	0.11	0.1075	1.68	0.28	1.34	0.16	1.34	0.16	0.0041	<0.0001	0.9023
	SYAM	1.23	0.09	1.17	0.10	0.1585	1.39	0.15	1.44	0.25	1.41	0.17	0.6288	0.7181	0.7191
	SYWM	1.19	0.07	1.23	0.16	0.4729	1.46	0.22	1.61	0.28	1.39	0.14	0.2097	0.2055	0.0015
	SYCM	1.21	0.19	1.11	0.08	0.2452	1.51	0.22	1.35	0.11	1.41	0.25	0.0498	0.2532	0.4708
	SYDM	1.19	0.12	1.12	0.10	0.1845	1.44	0.19	1.38	0.11	1.50	0.25	0.4212	0.4976	0.1619
	SYYM	1.16	0.12	1.14	0.10	0.7951	1.66	0.16	1.47	0.14	1.43	0.15	0.0107	0.0002	0.5526
	SYTM	1.32	0.15	1.03	0.10	0.0006	1.49	0.15	1.32	0.11	1.54	0.26	0.0090	0.5886	0.0112
	SYFM	1.21	0.24	1.12	0.32	0.5300	1.36	0.28	1.37	0.20	1.39	0.17	0.9908	0.6702	0.6770
	SYSM	1.22	0.07	1.12	0.05	0.0047	1.49	0.05	1.39	0.10	1.43	0.12	0.0074	0.1266	0.3025
	ALBU	1.01	0.79	1.64	0.54	0.0967	0.46	0.14	1.57	0.44	1.72	0.47	<0.0001	<0.0001	0.3594
	CO3	1.26	0.42	1.21	0.23	0.7725	1.06	0.10	1.25	0.24	1.60	0.35	0.0374	<0.0001	0.0053
	CO5	1.23	0.22	1.13	0.15	0.2998	1.27	0.14	1.38	0.14	1.44	0.21	0.1028	0.0167	0.3369
	MBL2	1.47	0.51	0.80	0.08	0.0059	1.70	0.50	1.57	0.33	1.38	0.29	0.4725	0.0121	0.0865
	HPT	1.40	0.74	0.76	0.19	0.0579	2.28	1.03	1.23	0.19	1.37	0.49	0.0055	0.0003	0.3954
	CO8B	1.25	0.38	1.18	0.05	0.6582	1.28	0.19	1.41	0.15	1.50	0.14	0.1045	0.0002	0.0777
	CO9	1.32	0.23	1.04	0.09	0.0112	1.34	0.22	1.38	0.37	1.50	0.21	0.7512	0.0504	0.2200
	A1AG2	1.38	0.46	0.89	0.12	0.0219	1.69	0.48	1.30	0.29	1.46	0.43	0.0403	0.1589	0.2627
	RET4	1.25	0.25	1.17	0.32	0.5295	1.09	0.20	1.16	0.18	1.85	0.89	0.4558	0.0111	0.0196

(*table continues*)

Table 2 (*continued*)

Variable	Protein	Test cohort					Validation cohort								
		Con		AH		Con vs AH	Con		AC		AH		Con vs AC	Con vs AH	AC vs AH
		Mean	SD	Mean	SD	*P* value	Mean	SD	Mean	SD	Mean	SD	*P* value		
Neutrophils	ELNE	1.08	0.40	1.40	0.51	0.1592	1.11	0.14	1.08	0.29	1.63	0.69	0.7984	0.0239	0.0201
	CAMP	1.07	0.16	1.52	0.42	0.0045	0.79	0.22	1.00	0.20	1.54	0.58	0.0375	0.0003	0.0068
	MPO	1.07	0.12	1.44	0.31	0.0025	0.94	0.09	0.93	0.17	1.72	0.70	0.8291	0.0012	0.0011
	BPI	0.90	0.10	1.82	0.53	<0.0001	1.14	0.17	1.11	0.32	1.60	0.75	0.7669	0.0683	0.0535
	MMP9	0.99	0.17	1.58	0.58	0.0041	1.15	0.10	1.04	0.12	1.65	0.59	0.0455	0.0112	0.0026
	CAP7	1.06	0.19	1.44	0.35	0.0080	1.15	0.16	1.12	0.20	1.70	0.62	0.6961	0.0092	0.0065
	PADI2	1.09	0.16	1.58	0.41	0.0019	1.22	0.10	1.21	0.05	1.78	0.54	0.9998	0.2847	0.0598
	PADI4	1.07	0.11	1.48	0.48	0.0096	1.00	0.10	1.07	0.18	1.64	0.52	0.3409	0.0004	0.0014
CL synthesis	LGAT1	1.23	0.39	1.10	0.17	0.4365	1.63	0.27	1.38	0.16	1.45	0.20	0.0222	0.0290	0.2957
	PLCB	1.31	0.28	0.96	0.22	0.0177	1.91	0.27	1.45	0.31	1.31	0.22	0.0025	<0.0001	0.1200
	LCLT1	ND	ND	ND	ND	ND	1.54	0.28	1.43	0.15	1.40	0.19	0.3136	0.1174	0.7381
	LPIN1	1.27	0.25	1.01	0.05	0.0263	2.02	0.49	1.39	0.38	1.42	0.32	0.0631	0.0051	0.8535
	TRIA1	1.24	0.17	1.01	0.08	0.0059	1.39	0.39	1.29	0.12	1.62	0.34	0.4497	0.0743	0.0047
	AGK	1.17	0.13	1.28	0.14	0.1089	1.56	0.14	1.49	0.14	1.44	0.15	0.3004	0.0339	0.3346
	TAM41	1.12	0.11	1.11	0.12	0.9505	1.19	0.19	1.23	0.14	1.46	0.12	0.6156	<0.0001	<0.0001
	PGS1	1.34	0.41	1.13	0.33	0.1254	1.42	0.16	1.49	0.24	1.57	0.36	0.9532	0.6428	0.9291
	PTPMT1	1.20	0.22	1.01	0.22	0.1065	1.90	0.51	1.61	0.24	1.28	0.19	0.1162	<0.0001	<0.0001
	ECHA	1.29	0.20	1.07	0.24	0.0546	1.91	0.18	1.33	0.18	1.40	0.27	<0.0001	<0.0001	0.4281
	PA2GA	1.37	1.44	0.69	0.23	0.2751	2.23	2.54	1.45	0.52	1.06	0.34	0.3555	0.0105	0.0072

AC, alcohol-associated cirrhosis; AH, alcohol-associated hepatitis; CL, cardiolipin; Con, control; ND, not detected.

$r = 0.4325$, $P = 0.01$; ASPN, $r = 0.4273$, $P = 0.01$) and Maddrey discriminant function score (FBLN3, $r = 0.4474$, $P = 0.008$; ASPN, $r = 0.5611$, $P = 0.0006$; LAMB1, $r = 0.3415$, $P = 0.05$) (Figure 4A, Supplemental Table S4), resulting in some discrimination across AH severity, as demonstrated by receiver operating characteristic analysis (Supplemental Table S12). With respect to phosphoregulation, only MECP2 had detectable phosphorylation at S80, an activation mark,[28] which was reduced in both AH cohorts (Figure 4B and Supplemental Figure S4A). Interestingly, alkaline phosphatase (ALPL), a phosphatase for pS80-MECP2,[29] was elevated in both AH cohorts relative to controls and AC (Figure 4B and Supplemental Figure S4B). Furthermore, elevated ALPL expression was maintained across AH severity, whereas pS80-MECP2 levels declined (Figure 4C). In AH nonsurvivors versus survivors, MECP2 levels were unchanged (Figure 4D), whereas pS80-MECP2 levels were reduced (Figure 4E).

Alterations in the Hepatic Protein Synthesis Process in AH and AC Elevate ALBU Expression but Not Its Phosphorylation

Patients with advanced liver diseases, including AH and AC, present clinically with reduced plasma albumin, long considered a result of decreased protein synthesis in the liver.[30] Indeed, many aspects and proteins involved in the protein synthesis machinery were down-regulated in AH and AC (Supplemental Figure S2B and Table 2). This effect did not appear to be driven by enhanced protein degradation because many proteasomal proteins [eg, proteasome subunit 20S subunit alpha 1 (PSA1) and proteasome subunit 20S subunit beta 5 (PSB5)] were down-regulated in AC and AH (Supplemental Tables S3 and S5). Within the protein synthesis processes, proteins significantly decreased in both AH cohorts and AC relative to controls were identified, including isoleucyl-TRNA synthetase 1 (SYIC), seryl-TRNA synthetase 1 (SYSC), alanyl-TRNA synthetase 1 (SYAC) (tRNA aminoacylation), isoleucyl-TRNA synthetase 2, mitochondrial (SYIM) (mt tRNA aminoacylation), and eukaryotic translation initiation factor 4 gamma 1 (IF4G1) (translational complex) (Table 2). As shown in Figure 5A and Supplemental Table S8, several proteins had significant negative associations with both MELD and Maddrey discriminant function scores [eg, eukaryotic translation elongation factor 2 (EF2), glutamyl-prolyl-TRNA synthetase 1 (SYEP), and asparaginyl-TRNA synthetase 2, mitochondrial (SYNM); MELD, Pearson $r = -0.3582$, -0.3723, and -0.3782, respectively; and Maddrey discriminant function, $r = -0.3392$, -0.4295, and -0.4523, respectively]. Changes in the protein synthesis machinery negatively impacted the levels of APPs (Table 2), most of which had significant negative associations with MELD score (Figure 5A). Figure 5, B and C, shows the pattern of protein expression across AH severity with the expression of valyl-TRNA synthetase 1 (SYVC) and complement C3 and C5 (CO3 and CO5, respectively)
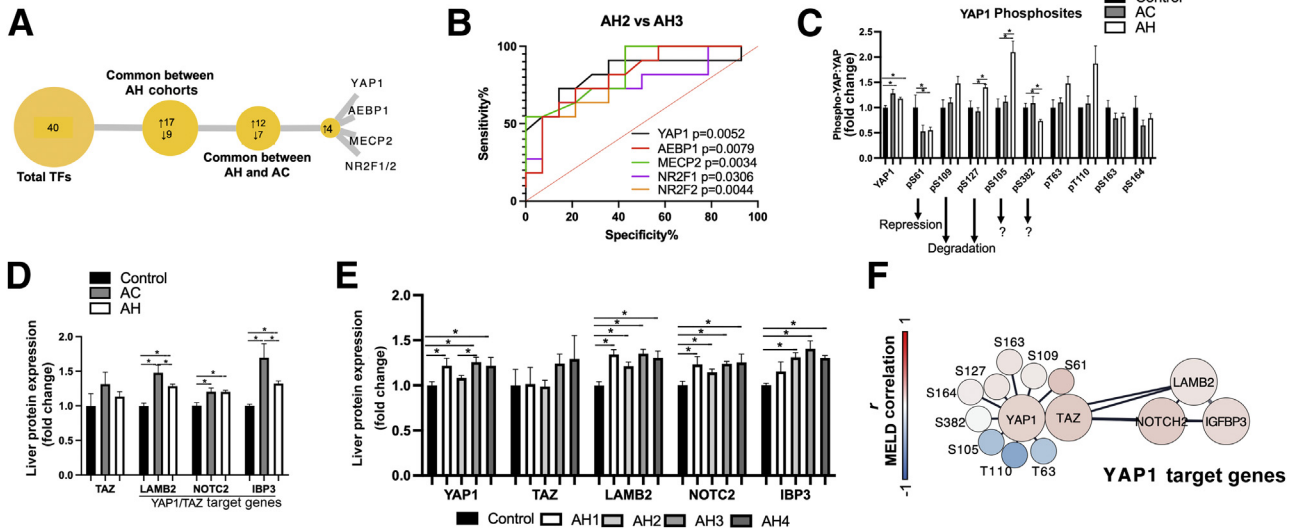
Figure 3   Up-regulated hepatic Yes1-associated transcriptional regulator (YAP1) expression is associated with compromised YAP1 phosphoregulation in alcohol-associated cirrhosis (AC) and alcohol-associated hepatitis (AH). **A:** Elevated transcription factors (TFs) common in both AH and AC cohorts. **B:** Receiver operating characteristic analysis for the AH2 versus AH3 comparison for YAP1, AE binding protein 1 (AEBP1), methyl-CpG binding protein 2 (MECP2), and nuclear receptor subfamily 2 group F members 1/2 (NR2F1/2) expression. **C:** Hepatic YAP1 and phosphorylated YAP1 levels in AC and AH patients. **D** and **E:** The expression of YAP1, WW domain containing transcription regulator 1 (TAZ), and YAP1 target genes laminin subunit beta 2 (LAMB2), Notch receptor 2 (NOTC2), and insulin-like growth factor binding protein 3 (IBP3) in AC and AH, and across AH severity. **F:** Correlation of TAZ, YAP1, YAP1 target genes, and YAP1 phosphosites with Model for End-Stage Liver Disease (MELD) score (node color corresponds to Pearson r value). Data are presented as means $\pm$ SEM (**C**–**E**). *$P < 0.05$ was considered significant.

being higher in AH1 compared with AH4. When further evaluating the functional output of hepatic protein synthesis, ALBU levels were unexpectedly elevated in both AH and AC (Figure 5D and Supplemental Figure S5A), which was confirmed by Western blot analysis in the liver tissue samples from the AH test cohort (Supplemental Figure S5,
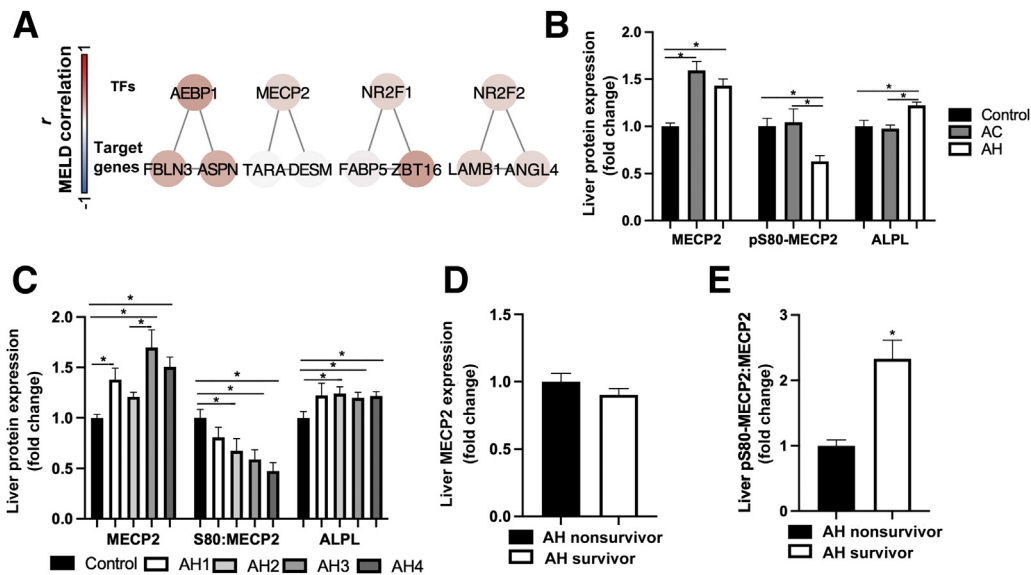
Figure 4   Elevated liver methyl-CpG binding protein 2 (MECP2) protein levels are associated with reduced phosphorylation in alcohol-associated hepatitis (AH). **A:** Correlation of profibrotic transcription factors (TFs) and their respective target genes with Model for End-Stage Liver Disease (MELD) score (node color corresponds to Pearson r value). **B:** MECP2, pS80-MECP2, and alkaline phosphatase biomineralization associated (ALPL) levels in alcohol-associated cirrhosis (AC) and AH. **C:** MECP2, pS80-MECP2, and ALPL levels across AH severity. **D** and **E:** MECP2 and pS80-MECP2:MECP2 levels for AH nonsurvivors relative to survivors. Data are presented as means $\pm$ SEM (**B**–**E**). *$P < 0.05$ was considered significant.
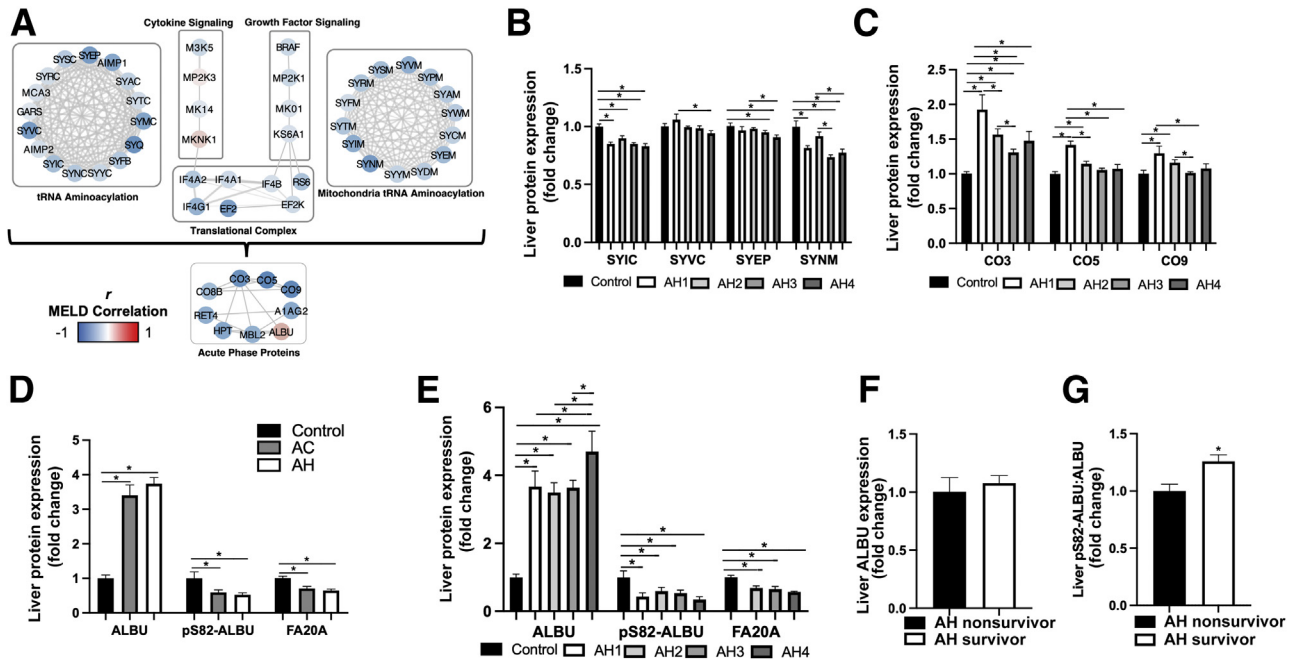
Figure 5 Alterations in the hepatic protein synthesis process in alcohol-associated hepatitis (AH) and alcohol-associated cirrhosis (AC): elevated albumin (ALBU) expression but not its phosphorylation. **A:** Correlation of the protein synthesis components and acute-phase proteins (APPs) with Model for End-Stage Liver Disease (MELD) score (node color corresponds to Pearson r value). **B** and **C:** Expression of protein synthesis components [isoleucyl-tRNA synthetase 1 (SYIC), valyl-tRNA synthetase 1 (SYVC), glutamyl-prolyl-tRNA synthetase 1 (SYEP), and asparaginyl-tRNA synthetase 2, mitochondrial (SYNM)] and APPs [complement C3 (CO3), complement C5 (CO5), and complement C9 (CO9)] across AH severity, respectively. **D:** ALBU, pS82-ALBU, and family with sequence similarity 20, member A (FA20A), levels in AC and AH. **E:** ALBU, pS82-ALBU, and FA20A levels across AH severity. **F** and **G:** ALBU and pS82-ALBU:ALBU levels in AH nonsurvivors relative to survivors. Data are presented as means ± SEM (**B–G**). *$P < 0.05$ was considered significant.

B and C). However, phosphorylation of ALBU at S82 (pS82-ALBU, a modification that facilitates ALBU secretion) was reduced in both the AH test and validation cohorts and in AC patients (Figure 5D and Supplemental Figure S5, D and E), as well as the expression of FA20A, the allosteric activator of FAM20C (the kinase responsible for pS82-ALBU phosphorylation).[31] FA20A and pS82-ALBU were unchanged across AH severity, whereas ALBU had the highest expression in the AH4 group (Figure 5E). More importantly, surviving AH patients had similar ALBU levels (Figure 5F) relative to nonsurviving patients with AH, but higher pS82-ALBU levels (Figure 5G). Lastly, no changes in the expression of the Fc gamma receptor and transporter (FCGRN), a hepatocellular receptor responsible for the uptake of ALBU, were observed in AC and AH and across AH severity (Supplemental Figure S6).

Hepatic Neutrophil-Related Proteins Are Elevated in Early AH but Reduced with AH Severity

Several APPs that were up-regulated in AH (CO3 and CO5) function as chemoattractants for neutrophils.[32] Given that neutrophil-related processes were also generally elevated in AH patients (Supplemental Figure S2A), the study aimed to further investigate neutrophil-related proteins. The expression of several proteins enriched in

neutrophils, including cathelicidin antimicrobial peptide, myeloperoxidase (MPO), matrix metallopeptidase 9, azurocidin 1 (CAP7), and peptidyl arginine deiminase 4, were significantly up-regulated in both AH cohorts, although there were limited changes in AC (Table 2). Interestingly, the expression of neutrophil proteins peaked at AH2 with a subsequent decline, suggesting that patients with more severe AH may have fewer hepatic neutrophils (Figure 6A). In the blood, the percentage of neutrophils was inversely related to AH severity, declining from AH1 to AH3, but with an increase in AH4 (Figure 6B). With respect to mortality, only MPO and CAP7 were higher in surviving patients with AH relative to nonsurviving patients with AH (Figure 6, C and D).

Compromised Hepatic Cardiolipin Biosynthesis in AC and AH

Hepatic mitochondrial dysfunction is a hallmark of ALD.[33] Our analysis identified that among the proteins down-regulated in AH was a subset involved in the synthesis of cardiolipin (CL) (Table 2), a phospholipid that maintains mitochondria bioenergetics[34] during hepatocyte proliferation and liver regeneration.[35] Figure 7A summarizes the CL biosynthesis pathway and shows the
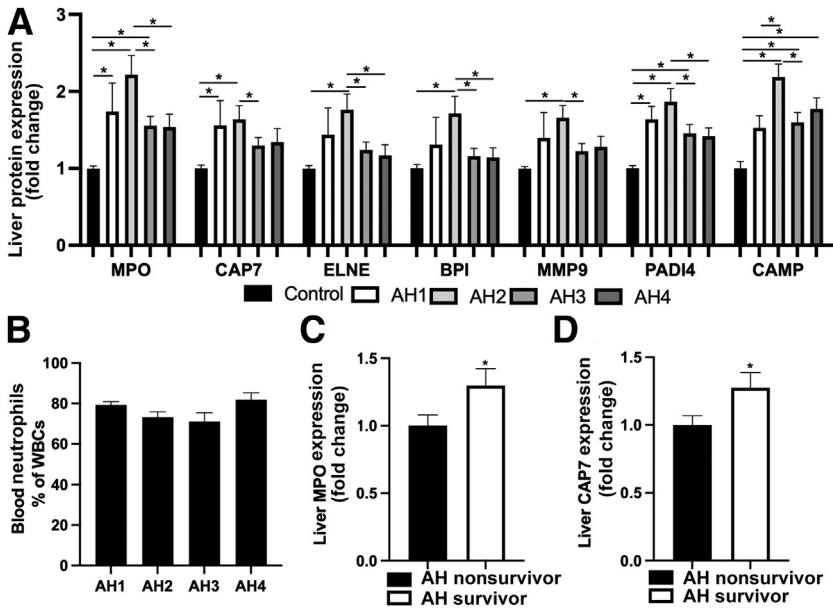
Figure 6 Hepatic neutrophil-related proteins are elevated in early alcohol-associated hepatitis (AH) but reduced with AH severity. **A:** Neutrophil protein expression [myeloperoxidase (MPO), azurocidin 1 (CAP7), elastase, neutrophil expressed (ELNE), bactericidal permeability increasing protein (BPI), matrix metallopeptidase 9 (MMP9), peptidyl arginine deiminase 4 (PADI4), and cathelicidin antimicrobial peptide (CAMP)] across AH severity. **B:** Whole blood neutrophils across AH severity [presented as a percentage of white blood cells (WBCs)]. **C** and **D:** Expression of MPO and CAP7 in AH nonsurvivors versus survivors. Data are presented as means ± SEM (**A–D**). *$P < 0.05$ was considered significant.

primarily negative correlation between MELD score and enzymes in this pathway, including critical proteins 1-acylglycerol-3-phosphate O-acyltransferase 2 (PLCB), protein tyrosine phosphatase mitochondrial 1 (PTPMT1), and hydroxyacyl-CoA dehydrogenase trifunctional complex subunit alpha (ECHA).[36] PLCB and PTPMT1 expression was slightly elevated from AH1 to AH2 but declined from AH2 to AH3 (PLCB being significant), whereas ECHA significantly declined from AH1 to AH3 (Figure 7B). As a consequence of the reduced levels of enzymes responsible for CL synthesis, liver CL levels were significantly reduced in AH and AC versus controls (−1.3-fold and −2.9-fold, respectively). Of note, CL levels in AH were significantly lower than in AC (−2.2-fold) (Figure 7C).

Discussion

In the current study, coupled hepatic proteomic and phosphoproteomic analysis in AC and AH patients revealed protein signatures specific to these disease states and to the stages of AH severity. One of the key observations from this study was that expression levels of the TF, YAP1, as well as YAP1 target genes were elevated in AC and AH and positively associated with AH severity. This is consistent with two recent studies demonstrating aberrant YAP1 activation contributing to hepatocyte transdifferentiation[26] and YAP1-mediated hepatocellular reprogramming, resulting in deficient hepatocyte maturation in AH.[37] However, the exact mechanisms of YAP1 up-regulation in AH remained unclear. One of the
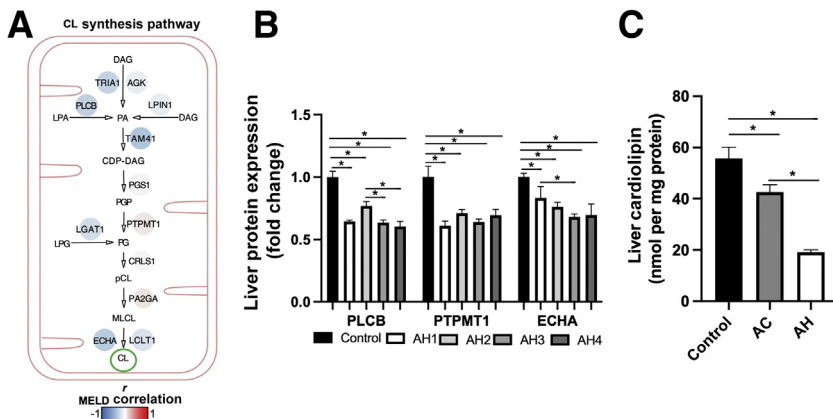

Figure 7 Alterations in the hepatic cardiolipin biosynthesis in alcohol-associated cirrhosis (AC) and alcohol-associated hepatitis (AH). **A:** The mitochondrial cardiolipin (CL) synthetic pathway and its correlation with Model for End-Stage Liver Disease (MELD) score (node color corresponds to Pearson r value) in AH validation cohort. **B:** Expression of 1-acylglycerol-3-phosphate O-acyltransferase 2 (PLCB), protein tyrosine phosphatase mitochondrial 1 (PTPMT1), and hydroxyacyl-CoA dehydrogenase trifunctional multienzyme complex subunit α (ECHA) across AH severity. **C:** Liver levels of cardiolipin in AC and AH patients. Data are presented as means ± SEM (**B** and **C**). *$P < 0.05$ was considered significant.

mechanisms of YAP1 regulation is its phosphorylation. It has been shown that pS127-YAP1 leads to proteasomal degradation of YAP1.[27] However, elevated levels of both pS127-YAP1 and YAP1 were observed in AH, suggesting that proteasomal degradation of YAP1 is likely compromised, possibly due to reduced expression of proteasome enzymes (eg, PSA1 and PSB5) or due to other degradation pathways (eg, autophagy, which is known to be compromised in AH).[38,39] Other known YAP1 phosphosites (eg, pS382-YAP1 and pS105-YAP1) with yet to be determined functions may also regulate YAP1 stability, although these modifications need to be studied further. Notably, the disease state and cell-specific expression of YAP1 are important considerations for its function. For example, in AH patients, YAP1 activation in hepatocytes prevents hepatocyte maturation, compromising their normal function,[26,37] whereas YAP1 activation in hepatic stellate cells facilitates liver fibrosis.[40,41] Aside from YAP1, other profibrotic TFs (namely, AEBP1, MECP2, NR2F1, and NR2F2) were also elevated in AH and AC and were positively associated with AH severity. These TFs had not previously been implicated in liver fibrosis in AH or AC, but were associated with liver fibrosis in human fatty liver disease,[42,43] hepatitis C—related cirrhosis,[44] and experimental rodent models.[28,44] Interestingly, although MECP2 expression was elevated, its activity (pS80-MECP2) was reduced in AH, possibly due to increased ALPL, a phosphatase that mediates the dephosphorylation of many substrates, including pS80-MECP2.[29] Because MECP2 is a transcriptional repressor,[45] loss of its activity may contribute to altered gene expression. MECP2 activity was only reduced in AH but not AC, indicating some differential function of MECP2 in these disease states.

Another process that was altered in AH and AC was protein synthesis, a critical hepatic function commonly compromised in chronic liver diseases, leading to hypoalbuminemia.[30] In this study, liver ALBU expression was elevated in AC and AH, but pS82-ALBU levels were reduced. Recent evidence suggests that phosphorylation of ALBU at S82 facilitates its secretion, and that FA20A/C is the responsible kinase complex for this process.[31] In addition, kinase inhibitors prevent ALBU secretion from hepatocytes,[46] further suggesting that ALBU phosphorylation is necessary for its release. The expression of the FA20A subunit of this complex was decreased in AC and AH, likely contributing to the reduction in pS82-ALBU, potentially explaining the hypoalbuminemia in patients with ALD.[30] Another possible mechanism regulating blood ALBU levels may be increased hepatocellular uptake of ALBU. However, there was no observed change in the expression of one ALBU uptake receptor, FCGRN, suggesting that loss of pS82-ALBU is likely the major mechanism. A recent study demonstrated that albumin infusions in cirrhosis patients (90% AC) have no beneficial effect on mortality,[47] but the effects of elevating systemic ALBU levels via other strategies (eg, increasing pS82-

ABLU to facilitate hepatocellular release) has not been evaluated. Similar to ALBU, other APPs (eg, CO3, CO5, and complement C9) were elevated in AH compared with controls, but as AH severity progressed, levels of these APPs declined. Similar to that in liver, elevated plasma CO5 levels in AH were also found to be reduced with increasing severity.[48] In addition to their bactericidal function, complement proteins CO3 and CO5 can also serve as neutrophil chemoattractants.[49] Loss of these proteins with AH progression could reduce neutrophil trafficking to the liver in patients with severe AH. Indeed, many neutrophil proteins (eg, MPO and CAP7) were elevated in AH patients with MELD scores between 17 and 25 but were decreased in patients with MELD scores of >25. Of note, neutrophil function in patients with AH is compromised,[50] and increased hepatic neutrophil infiltration is associated with enhanced 90-day survival probability.[51] A known therapy that stimulates neutrophil production (eg, granulocyte colony-stimulating factor) has produced mixed results in clinical trials for patients with AH.[9] The study data suggest that the loss of chemoattractants in later stages of AH may contribute to the ineffectiveness of granulocyte colony-stimulating factor therapy. Lastly, maladaptive changes in liver metabolism were also identified in this study, including a reduction in CL synthesis enzymes and CL levels in AC and AH. In addition to enhanced CL oxidation,[52] a reduction in CL synthesis could compromise mitochondrial function[33] (eg, mt biogenesis), leading to alterations in liver function, including regeneration.[35]

Although this study is unique in many ways, the approach had several limitations, including study cohorts being primarily comprised of men, limiting the ability to evaluate sex differences. This study was cross-sectional and did not observe patients over time. Another limitation was that the classification of AH severity groups was based on MELD score and was somewhat arbitrary. Similarly, designation of AC was based on the presence of cirrhosis with no histologic evidence of hepatitis. Although the therapeutic regimens were not evaluated as a factor contributing to proteome changes, that would be of interest for future studies. Lastly, proteome and phosphoproteome changes were representative of the whole liver and not of individual cell types.

In summary, this is a novel study that used two independent AH cohorts, which yielded reproducible patterns of protein expression in the liver. The first cohort was a series of patients undergoing liver transplant (explant tissue) on the US East coast, and the second (validation) cohort was from a broader spectrum of patients with AH undergoing liver biopsy in the US West coast (specifically in California). An additional strength of the study was the in-depth analysis of proteome and phosphoproteome changes across the spectrum of AH severity and AH versus AC. The study uniquely applied coupled hepatic proteome and phosphoproteome analyses

to identify similarities and differences in AC and AH and further delineate mechanistic insights into AH development and progression. Major findings of this research included a novel mechanism of YAP1 dysregulation, compromised ALBU phosphorylation (possibly preventing hepatic ALBU release, contributing to hypoalbuminemia), and diminished CL synthesis (likely exacerbating mitochondria dysfunction) (graphical abstract). These results pave the way for further studies to evaluate the potential of these findings in developing targeted therapeutic strategies.

Acknowledgments

Author Contributions

I.K., J.J., C.M., T.M., A.S., J.H., and L.D. conceptualized the study; J.J., L.D., M.G., and J.H. developed methodology; L.D., M.G., and J.H. performed software analysis; J.J., L.D., and J.H. performed formal analysis; I.K., C.M., J.J., L.D., and J.H. conducted investigations; I.K., J.J., C.M., M.G., T.M., and A.S. provided resources; J.J., L.D., A.A., and J.H. curated data; J.H., L.D., C.M., and I.K. wrote the original draft of the manuscript; I.K., J.J., C.M., T.M., J.H., L.D., J.W., D.W., A.A., M.G., and A.S. reviewed and edited the manuscript; J.H., L.D., and J.W. performed visualization; I.K. and J.J. supervised the project; I.K., J.J., T.M., C.M., and A.S. contributed to project administration; I.K., C.M., J.J., T.M., A.S., J.H., and J.W acquired funding. All authors have reviewed and approved the manuscript.

Supplemental Data

Supplemental material for this article can be found at *http://doi.org/10.1016/j.ajpath.2022.04.004*.

References

1. Asrani SK, Devarbhavi H, Eaton J, Kamath PS: Burden of liver diseases in the world. J Hepatol 2019, 70:151–171
2. Young-Hee Yoon CMC: Liver Cirrhosis Mortality in the United States: National, State, and Regional Trends, 2000-2017. Hyattsville, MD: US Department of Health and Human Services, National Institutes of Health, 2019. pp. 1–88
3. O'Shea RS, Dasarathy S, McCullough AJ: Alcoholic liver disease. Hepatology 2010, 51:307–328
4. Lucey MR, Mathurin P, Morgan TR: Alcoholic hepatitis. N Engl J Med 2009, 360:2758–2769
5. Michelena J, Altamirano J, Abraldes JG, Affò S, Morales-Ibanez O, Sancho-Bru P, Dominguez M, García-Pagán JC, Fernández J, Arroyo V, Ginès P, Louvet A, Mathurin P, Mehal WZ, Caballería J, Bataller R: Systemic inflammatory response and serum lipopolysaccharide levels predict multiple organ failure and death in alcoholic hepatitis. Hepatology 2015, 62:762–772
6. NIAAA: Alcohol Sales During the COVID-19 Pandemic. Bethesda, MD: National Institute on Alcohol Abuse and Alcoholism, 2021
7. Rutledge SM, Schiano TD, Florman S, Im GY: COVID-19 aftershocks on alcohol-associated liver disease: an early cross-sectional report from the U.S. epicenter. Hepatol Commun 2021, 5: 1151–1155
8. Moon AM, Curtis B, Mandrekar P, Singal AK, Verna EC, Fix OK: Alcohol-associated liver disease before and after COVID-19-an overview and call for ongoing investigation. Hepatol Commun 2021, 5:1616–1621
9. Singal AK, Shah VH: Current trials and novel therapeutic targets for alcoholic hepatitis. J Hepatol 2019, 70:305–313
10. Innes H, Buch S, Hutchinson S, Guha IN, Morling JR, Barnes E, Irving W, Forrest E, Pedergnana V, Goldberg D, Aspinall E, Barclay S, Hayes PC, Dillon J, Nischalke HD, Lutz P, Spengler U, Fischer J, Berg T, Brosch M, Eyer F, Datz C, Mueller S, Peccerella T, Deltenre P, Marot A, Soyka M, McQuillin A, Morgan MY, Hampe J, Stickel F: Genome-wide association study for alcohol-related cirrhosis identifies risk loci in MARC1 and HNRNPUL1. Gastroenterology 2020, 159:1276–1289.e7
11. Beaudoin JJ, Long N, Liangpunsakul S, Puri P, Kamath PS, Shah V, Sanyal AJ, Crabb DW, Chalasani NP, Urban TJ: An exploratory genome-wide analysis of genetic risk for alcoholic hepatitis. Scand J Gastroenterol 2017, 52:1263–1269
12. Argemi J, Latasa MU, Atkinson SR, Blokhin IO, Massey V, Gue JP, et al: Defective HNF4alpha-dependent gene expression as a driver of hepatocellular failure in alcoholic hepatitis. Nat Commun 2019, 10: 3126
13. Massey V, Parrish A, Argemi J, Moreno M, Mello A, García-Rocha M, Altamirano J, Odena G, Dubuquoy L, Louvet A, Martinez C, Adrover A, Affò S, Morales-Ibanez O, Sancho-Bru P, Millán C, Alvarado-Tapias E, Morales-Arraez D, Caballería J, Mann J, Cao S, Sun Z, Shah V, Cameron A, Mathurin P, Snider N, Villanueva C, Morgan TR, Guinovart J, Vadigepalli R, Bataller R: Integrated multiomics reveals glucose use reprogramming and identifies a novel hexokinase in alcoholic hepatitis. Gastroenterology 2021, 160:1725–1740.e2
14. Warner D, Vatsalya V, Zirnheld KH, Warner JB, Hardesty JE, Umhau JC, McClain CJ, Maddipati K, Kirpich IA: Linoleic acid-derived oxylipins differentiate early stage alcoholic hepatitis from mild alcohol-associated liver injury. Hepatol Commun 2021, 5: 947–960
15. Duan Y, Llorente C, Lang S, Brandl K, Chu H, Jiang L, et al: Bacteriophage targeting of gut bacterium attenuates alcoholic liver disease. Nature 2019, 575:505–511
16. Diamond DL, Proll SC, Jacobs JM, Chan EY, Camp DG 2nd, Smith RD, Katze MG: HepatoProteomics: applying proteomic

technologies to the study of liver function and disease. Hepatology 2006, 44:299–308

17. Wang Y, Yang F, Gritsenko MA, Wang Y, Clauss T, Liu T, Shen Y, Monroe ME, Lopez-Ferrer D, Reno T, Moore RJ, Klemke RL, Camp DG 2nd, Smith RD: Reversed-phase chromatography with multiple fraction concatenation strategy for proteome profiling of human MCF10A cells. Proteomics 2011, 11:2019–2026

18. Mertins P, Tang LC, Krug K, Clark DJ, Gritsenko MA, Chen L, Clauser KR, Clauss TR, Shah P, Gillette MA, Petyuk VA, Thomas SN, Mani DR, Mundt F, Moore RJ, Hu Y, Zhao R, Schnaubelt M, Keshishian H, Monroe ME, Zhang Z, Udeshi ND, Mani D, Davies SR, Townsend RR, Chan DW, Smith RD, Zhang H, Liu T, Carr SA: Reproducible workflow for multiplexed deep-scale proteome and phosphoproteome analysis of tumor tissues by liquid chromatography-mass spectrometry. Nat Protoc 2018, 13: 1632–1661

19. Zhang H, Liu T, Zhang Z, Payne SH, Zhang B, McDermott JE, et al: Integrated proteogenomic characterization of human high-grade serous ovarian cancer. Cell 2016, 166:755–765

20. Elias JE, Gygi SP: Target-decoy search strategy for increased confidence in large-scale protein identifications by mass spectrometry. Nat Methods 2007, 4:207–214

21. Qian WJ, Liu T, Monroe ME, Strittmatter EF, Jacobs JM, Kangas LJ, Petritis K, Camp DG 2nd, Smith RD: Probability-based evaluation of peptide and protein identifications from tandem mass spectrometry and SEQUEST analysis: the human proteome. J Proteome Res 2005, 4:53–62

22. Kim S, Gupta N, Pevzner PA: Spectral probabilities and generating functions of tandem mass spectra: a strike against decoy databases. J Proteome Res 2008, 7:3354–3363

23. Hardesty JE, Warner JB, Song YL, Rouchka EC, McClain CJ, Warner DR, Kirpich IA: Ileum gene expression in response to acute systemic inflammation in mice chronically fed ethanol: beneficial effects of elevated tissue n-3 PUFAs. Int J Mol Sci 2021, 22:1582

24. Ernst J, Bar-Joseph Z: STEM: a tool for the analysis of short time series gene expression data. BMC Bioinformatics 2006, 7:191

25. Kamath PS, Wiesner RH, Malinchoc M, Kremers W, Therneau TM, Kosberg CL, D'Amico G, Dickson ER, Kim WR: A model to predict survival in patients with end-stage liver disease. Hepatology 2001, 33:464–470

26. Bou Saleh M, Louvet A, Ntandja-Wandji LC, Boleslawski E, Gnemmi V, Lassailly G, Truant S, Maggiotto F, Ningarhari M, Artru F, Anglo E, Sancho-Bru P, Corlu A, Argemi J, Dubois-Chevalier J, Dharancy S, Eeckhoute J, Bataller R, Mathurin P, Dubuquoy L: Loss of hepatocyte identity following aberrant YAP activation: a key mechanism in alcoholic hepatitis. J Hepatol 2021, 75:912–923

27. Zhao B, Li L, Tumaneng K, Wang CY, Guan KL: A coordinated phosphorylation by Lats and CK1 regulates YAP stability through SCF(beta-TRCP). Genes Dev 2010, 24:72–85

28. Moran-Salvador E, Garcia-Macia M, Sivaharan A, Sabater L, Zaki MYW, Oakley F, Knox A, Page A, Luli S, Mann J, Mann DA: Fibrogenic activity of MECP2 is regulated by phosphorylation in hepatic stellate cells. Gastroenterology 2019, 157: 1398–1412.e9

29. Gonzales ML, Adams S, Dunaway KW, LaSalle JM: Phosphorylation of distinct sites in MeCP2 modifies cofactor associations and the dynamics of transcriptional regulation. Mol Cell Biol 2012, 32: 2894–2903

30. Jagdish RK, Maras JS, Sarin SK: Albumin in advanced liver diseases: the good and bad of a drug! Hepatology 2021, 74: 2848–2862

31. Tagliabracci VS, Wiley SE, Guo X, Kinch LN, Durrant E, Wen J, Xiao J, Cui J, Nguyen KB, Engel JL, Coon JJ, Grishin N, Pinna LA, Pagliarini DJ, Dixon JE: A single kinase generates the majority of the secreted phosphoproteome. Cell 2015, 161:1619–1632

32. Price PJ, Bánki Z, Scheideler A, Stoiber H, Verschoor A, Sutter G, Lehmann MH: Complement component C5 recruits neutrophils in the absence of C3 during respiratory infection with modified vaccinia virus Ankara. J Immunol 2015, 194:1164–1168

33. Abdallah MA, Singal AK: Mitochondrial dysfunction and alcohol-associated liver disease: a novel pathway and therapeutic target. Signal Transduct Target Ther 2020, 5:26

34. Dudek J: Role of cardiolipin in mitochondrial signaling pathways. Front Cell Dev Biol 2017, 5:90

35. Webster J, Jiang JY, Lu B, Xu FY, Taylor WA, Mymin M, Zhang M, Minuk GY, Hatch GM: On the mechanism of the increase in cardiolipin biosynthesis and resynthesis in hepatocytes during rat liver regeneration. Biochem J 2005, 386:137–143

36. Falabella M, Vernon HJ, Hanna MG, Claypool SM, Pitceathly RDS: Cardiolipin, mitochondria, and neurological disease. Trends Endocrinol Metab 2021, 32:224–237

37. Hyun J, Sun Z, Ahmadi AR, Bangru S, Chembazhi UV, Du K, Chen T, Tsukamoto H, Rusyn I, Kalsotra A, Diehl AM: Epithelial splicing regulatory protein 2-mediated alternative splicing reprograms hepatocytes in severe alcoholic hepatitis. J Clin Invest 2020, 130: 2129–2145

38. Ding WX, Manley S, Ni HM: The emerging role of autophagy in alcoholic liver disease. Exp Biol Med (Maywood) 2011, 236: 546–556

39. Lee YA, Noon LA, Akat KM, Ybanez MD, Lee TF, Berres ML, Fujiwara N, Goossens N, Chou HI, Parvin-Nejad FP, Khambu B, Kramer EGM, Gordon R, Pfleger C, Germain D, John GR, Campbell KN, Yue Z, Yin XM, Cuervo AM, Czaja MJ, Fiel MI, Hoshida Y, Friedman SL: Autophagy is a gatekeeper of hepatic differentiation and carcinogenesis by controlling the degradation of Yap. Nat Commun 2018, 9:4962

40. Mannaerts I, Leite SB, Verhulst S, Claerhout S, Eysackers N, Thoen LF, Hoorens A, Reynaert H, Halder G, van Grunsven LA: The Hippo pathway effector YAP controls mouse hepatic stellate cell activation. J Hepatol 2015, 63:679–688

41. Konishi T, Schuster RM, Lentsch AB: Proliferation of hepatic stellate cells, mediated by YAP and TAZ, contributes to liver repair and regeneration after liver ischemia-reperfusion injury. Am J Physiol Gastrointest Liver Physiol 2018, 314: G471–G482

42. Elbel EE, Lavine JE, Downes M, Van Natta M, Yu R, Schwimmer JB, Behling C, Brunt EM, Tonascia J, Evans R: Hepatic nuclear receptor expression associates with features of histology in pediatric nonalcoholic fatty liver disease. Hepatol Commun 2018, 2: 1213–1226

43. Gerhard GS, Hanson A, Wilhelmsen D, Piras IS, Still CD, Chu X, Petrick AT, DiStefano JK: AEBP1 expression increases with severity of fibrosis in NASH and is regulated by glucose, palmitate, and miR-372-3p. PLoS One 2019, 14:e0219764

44. Ceni E, Mello T, Polvani S, Vasseur-Cognet M, Tarocchi M, Tempesti S, Cavalieri D, Beltrame L, Marroncini G, Pinzani M, Milani S, Galli A: The orphan nuclear receptor COUP-TFII coordinates hypoxia-independent proangiogenic responses in hepatic stellate cells. J Hepatol 2017, 66:754–764

45. Nan X, Campoy FJ, Bird A: MeCP2 is a transcriptional repressor with abundant binding sites in genomic chromatin. Cell 1997, 88:471–481

46. Webb RJ, Judah JD, Lo LC, Thomas GM: Constitutive secretion of serum albumin requires reversible protein tyrosine phosphorylation events in trans-Golgi. Am J Physiol Cell Physiol 2005, 289: C748–C756

47. China L, Freemantle N, Forrest E, Kallis Y, Ryder SD, Wright G, Portal AJ, Becares Salles N, Gilroy DW, O'Brien A: A randomized trial of albumin infusions in hospitalized patients with cirrhosis. N Engl J Med 2021, 384:808–817

48. Fan X, McCullough RL, Huang E, Bellar A, Kim A, Poulsen KL, McClain CJ, Mitchell M, McCullough AJ, Radaeva S, Barton B, Szabo G, Dasarathy S, Rotroff DM, Nagy LE: Diagnostic and

prognostic significance of complement in patients with alcohol-associated hepatitis. Hepatology 2021, 73:983−997

49. Metzemaekers M, Gouwy M, Proost P: Neutrophil chemoattractant receptors in health and disease: double-edged swords. Cell Mol Immunol 2020, 17:433−450

50. Mookerjee RP, Stadlbauer V, Lidder S, Wright GA, Hodges SJ, Davies NA, Jalan R: Neutrophil dysfunction in alcoholic hepatitis superimposed on cirrhosis is reversible and predicts the outcome. Hepatology 2007, 46:831−840

51. Altamirano J, Miquel R, Katoonizadeh A, Abraldes JG, Duarte-Rojo A, Louvet A, Augustin S, Mookerjee RP, Michelena J, Smyrk TC, Buob D, Leteurtre E, Rincón D, Ruiz P, García-Pagán JC, Guerrero-Marquez C, Jones PD, Barritt ASt, Arroyo V, Bruguera M, Bañares R, Ginès P, Caballería J, Roskams T, Nevens F, Jalan R, Mathurin P, Shah VH, Bataller R: A histologic scoring system for prognosis of patients with alcoholic hepatitis. Gastroenterology 2014, 146:1231−1239. e1-6

52. Rolla R, Vay D, Mottaran E, Parodi M, Vidali M, Sartori M, Rigamonti C, Bellomo G, Albano E: Antiphospholipid antibodies associated with alcoholic liver disease specifically recognise oxidised phospholipids. Gut 2001, 49:852−859